

## Stereochemical Effects

Evaluation of the Alicyclic *Gauche* Effect in 2-Fluorocyclohexanone Analogs: a Combined NMR and DFT StudyDaniela Rodrigues Silva,<sup>[a,b]</sup> Lucas A. Zeoly,<sup>[c]</sup> Rodrigo A. Cormanich,<sup>[c]</sup> Célia Fonseca Guerra,<sup>\*, [b,d]</sup> and Matheus P. Freitas<sup>\*[a]</sup>

**Abstract:** Herein, we have investigated the effect of an endocyclic group (forming the N–C–F fragment) on the conformational preferences of 2-fluorocyclohexanone analogs. A combined approach of nuclear magnetic resonance and density functional theory calculations was employed to assess the conformational equilibrium in several media. In turn, natural bond orbital analysis and the conformational behavior of other 2-halocyclohexanone analogs were used to get more insights about the intramolecular interactions governing the conformer

stabilities. Our results reveal that any stabilization from interactions featured in the *gauche* effect is overcome by a short-range interaction of the fluorine substituent with the carbonyl group. Consequently, the *gauche* effect in heterocyclic compounds is not as stabilizing as in their acyclic counterparts. Only the electrostatic *gauche* effect takes place even in polar solvents owing to an attraction between the axial fluorine and an endocyclic quaternary ammonium group.

## Introduction

The 2-fluorocyclohexanone moiety is a molecular building block of organic compounds with application in several research fields. It has a well-defined conformational equilibrium, in which the six membered ring undergoes chair inversion resulting in energy minimum conformations with either axial or equatorial fluorine atom (Figure 1) with a significant solvent dependence.<sup>[1]</sup> The axial fluorine is the most stable conformer in the gas phase, but the equilibrium gradually shifts towards the equatorial conformer with the increase of the solvent polarity. The equatorial conformer has a higher dipole moment and is naturally more stabilized by polar solvents. Nevertheless, this conformational preference has usually been attributed to an

interplay of intramolecular interactions involving the carbonyl group.<sup>[2]</sup> In the gas phase, there is a repulsion between the equatorial fluorine and the carbonyl group (the C–F and C=O bonds are almost parallel to each other in the same plane), forcing the fluorine to adopt an axial orientation. Insofar as the polarity of the solvent increases, the repulsion is attenuated and a charge transfer from the  $\sigma_{\text{CHax}}$  bond to the  $\pi^*_{\text{CO}}$  antibonding orbital overrides other interactions to favor the equatorial conformer (Figure 1).<sup>[2]</sup>

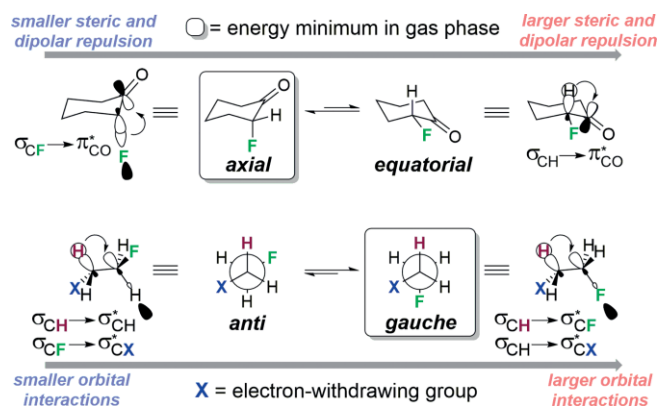


Figure 1. Schematic representation of the axial–equatorial equilibrium in the 2-fluorocyclohexanone (on the top) along with the *anti*–*gauche* equilibrium in the 1,2-disubstituted ethane (on the bottom).

The introduction of a fluorine atom in an organic molecule is known to impart predictable stereoelectronic effects that can change its conformational behavior; a compelling example is the *gauche* effect.<sup>[3]</sup> The *gauche* effect is observed in structures containing two bonded carbon atoms attached to vicinal elec-

[a] Departamento de Química, Universidade Federal de Lavras 37200-900, Lavras – MG, Brazil  
E-mail: matheus@ufla.br  
<https://molecc.wixsite.com/molecc>

[b] Theoretical Chemistry, Department of Chemistry and Pharmaceutical Sciences, AIMMS, Vrije Universiteit Amsterdam  
De Boelelaan 1083, 1081 HV Amsterdam, The Netherlands  
E-mail: c.fonseca Guerra@vu.nl  
<http://www.few.vu.nl/~guerra>

[c] Chemistry Institute, University of Campinas  
13083-970, Campinas – SP, Brazil

[d] Leiden Institute of Chemistry, Gorlaeus Laboratories, Leiden University  
Einsteinweg 55, 2333 CC Leiden, The Netherlands

Supporting information and ORCID(s) from the author(s) for this article are available on the WWW under <https://doi.org/10.1002/ejoc.201901815>.

© 2020 The Authors. Published by Wiley-VCH Verlag GmbH & Co. KGaA. This is an open access article under the terms of the Creative Commons Attribution-NonCommercial License, which permits use, distribution and reproduction in any medium, provided the original work is properly cited and is not used for commercial purposes.

tron withdrawing groups (in the form F–C–X for organofluorine compounds), in which the F and X preferentially adopt the *gauche* orientation ( $\varphi_{\text{F-C-X}} \approx 60^\circ$ ) instead of the *anti*-orientation ( $\varphi_{\text{F-C-X}} \approx 180^\circ$ ), Figure 1. The *gauche* preference has been commonly explained in terms of hyperconjugative interactions.<sup>[4]</sup> The destabilizing effect of bringing two electron rich groups close together is overcome by a greater stabilization from antiperiplanar orbital interactions. The best electron donor ( $\sigma_{\text{CH}}$  bond) and acceptor ( $\sigma_{\text{CF}}^*$  antibonding) orbitals are aligned in the *gauche* arrangement for the  $\sigma_{\text{CH}} \rightarrow \sigma_{\text{CF}}^*$  charge transfer, in contrast to the  $\sigma_{\text{CH}} \rightarrow \sigma_{\text{CH}}^*$  and  $\sigma_{\text{CF}} \rightarrow \sigma_{\text{CX}}^*$  in the *anti*-orientation (Figure 1).<sup>[5]</sup>

If compared with other intramolecular interactions (such as hydrogen bonds and electrostatic interactions), the *gauche* effect may have only a subtle effect on the conformational preferences of organic compounds.<sup>[3a]</sup> Nonetheless, its strength depends on the groups involved;<sup>[6]</sup> the *gauche-anti* energy difference in some fluoroethylamides, for example, can be of  $1.8 \text{ kcal mol}^{-1}$  in favor of the *gauche* conformer.<sup>[7]</sup> In fact, the *gauche* effect has been exploited as a conformational control strategy in the design of performance organic compounds in catalysis,<sup>[8]</sup> biological systems<sup>[9]</sup> and organometallic complexes.<sup>[10]</sup> With this in mind, we wonder if the introduction of an endocyclic group, such as a carbamate group, in the structure of the 2-fluorocyclohexanone could induce a conformational shift to further stabilize the axial fluorine due to the *gauche* effect. A recent report has suggested that the reactivity of some  $\alpha$ -fluoroketones may be related to their conformational preferences.<sup>[11]</sup> Therefore, a conformational induction in the 2-fluorocyclohexanone backbone could be used to modulate a desired molecular property, such as reactivity towards a specific reaction mechanism.<sup>[12]</sup>

In an initiative to induce a *gauche* effect in the backbone of the 2-fluorocyclohexanone, Silva et al.<sup>[13]</sup> introduced an oxygen atom in the six-membered ring in order to attain a *gauche* arrangement along the  $\text{O}_{\text{endo}}\text{-C-C-F}_{\text{ax}}$  fragment. However, it actually caused an incremental repulsion between oxygen and axial fluorine, which favored the equatorial conformer even in the gas phase. In the case of the endocyclic carbamate group envisaged here, it is expected a smaller repulsion because the endocyclic nitrogen atom is engaged in a resonance with the carbonyl group. Therefore, the stabilizing orbital interactions in the *gauche* arrangement would overcome other intramolecular interactions to favor the axial fluorine.

Thus, the conformational analysis of the 1-Boc-3-fluoro-4-oxopiperidine (**1**, Figure 2) is performed herein. Compound **1** has an endocyclic *N*-Boc group in the six membered ring that could result in a *gauche* orientation with the axial fluorine atom, instead of an *anti* orientation with equatorial fluorine. The Boc group acts as a protective group and **1** has been commonly employed as an intermediate in organic synthesis.<sup>[14]</sup> Therefore, this work aims at investigating whether the *N*-Boc group introduces intramolecular interactions (especially orbital interactions due to the *gauche* effect) that could cooperatively act with the carbonyl group to increase the fluorine axial preference, even in solution. For this, the energy minimum conformations of **1** and their population in different media were investigated by a

combined approach using nuclear magnetic resonance (NMR) and density functional theory (DFT) calculations, and then the prospective intramolecular interactions responsible for their relative stability were theoretically evaluated. In addition, the *N*-Boc group in **1** was successively replaced with other groups, as well as the fluorine at position 2 (see atom numbering in Figure 2), to theoretically find an optimal substituent activating the alicyclic *gauche* effect.

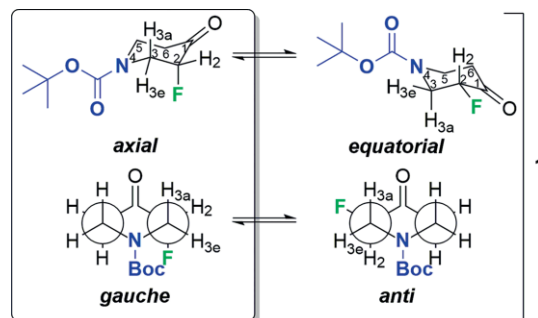


Figure 2. Conformational equilibrium of the 1-Boc-3-fluoro-4-oxopiperidine (**1**). The antiperiplanar interactions (i.e.  $\sigma_{\text{CH}} \rightarrow \sigma_{\text{CF}}^*$  and  $\sigma_{\text{CH}} \rightarrow \sigma_{\text{CN}}^*$ ) present in the *gauche* orientation of the endocyclic nitrogen with fluorine atom are expected to stabilize the axial conformer of **1**.

## Results and Discussion

The first step towards investigating the conformational landscape of **1** consisted in evaluating the orientation of the *N*-Boc group through rotation around the  $\text{N-C(=O)}$  bond. Due to the resonance in the carbamate group, it is expected a planar geometry along the  $\text{N-C(=O)-O}$  atoms and then two orientations for the Boc's carbonyl group with  $\varphi_{\text{C-N-C=O}}$  dihedral angle of about  $0^\circ$  and  $180^\circ$ . Thus, the energy profile at the MP2/6-311++G(d,p)<sup>[15]</sup> level for the axial and equatorial conformers of **1** as a function of the  $\varphi_{\text{C-N-C=O}}$  dihedral angle is shown in Figure 3 (the Cartesian coordinates of all structures are given in

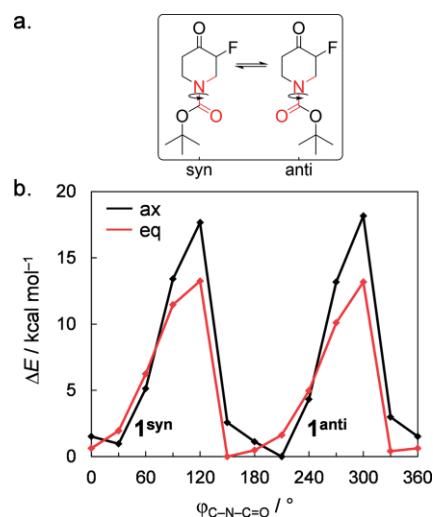


Figure 3. a) Schematic representation for the interconversion between conformers **1**<sup>syn</sup> and **1**<sup>anti</sup> through rotation of the  $\text{N-C(=O)}$  bond; b) energy profile for the rotation around the  $\varphi_{\text{C-N-C=O}}$  torsion angle with a step size of  $30^\circ$  at MP2/6-311++G(d,p) level for the axial (black curve) and equatorial (red curve) conformers of **1**.

the Supporting Information). Two energy minima (named **1<sup>syn</sup>** and **1<sup>anti</sup>**) were found for both conformers, as expected, in which the second one ( $\varphi_{C-N-C=O} \approx 180^\circ$ ) is somewhat more stable. The energy difference between them is small and more significant for the axial ( $\Delta E = 0.96 \text{ kcal mol}^{-1}$ ) than for the equatorial ( $\Delta E = 0.63 \text{ kcal mol}^{-1}$ ) conformation. Likewise, Figure 3 also shows two energy maxima, with the  $\varphi_{C-N-C=O}$  dihedral angle of  $120^\circ$  and  $300^\circ$  for both conformers. The interconversion barrier is higher for the axial form (ca.  $18 \text{ kcal mol}^{-1}$  compared to  $13 \text{ kcal mol}^{-1}$  in the equatorial form), probably because of the closer proximity between the axial fluorine and both oxygen atoms of the Boc group in the energy maximum structures.

The geometries of the four energy minima located in Figure 3 were then fully optimized using dispersion corrected B3LYP<sup>[16]</sup> according to the Becke and Johnson (BJ) damping function<sup>[17]</sup> with the 6-311++G(d,p) basis set.<sup>[15b]</sup> This level of theory was selected based on a benchmark study with MP2, see Experimental section and Table S1 in the Supporting Information for details. Interconversion between these four structures through sequential steps of N-C(=O) bond rotation and ring flipping forms the conformational cycle depicted in the Figure 4. The conformers have been labelled in the Figure 4 to distinguish the two orientations of the N-Boc group (**syn** and **anti**) and axial or equatorial fluorine (**ax** and **eq**, respectively), and the conformational equilibrium between these four structures (namely **1<sub>ax<sup>syn</sup></sub>**, **1<sub>ax<sup>anti</sup></sub>**, **1<sub>eq<sup>syn</sup></sub>**, **1<sub>eq<sup>anti</sup></sub>**) has been investigated herein.

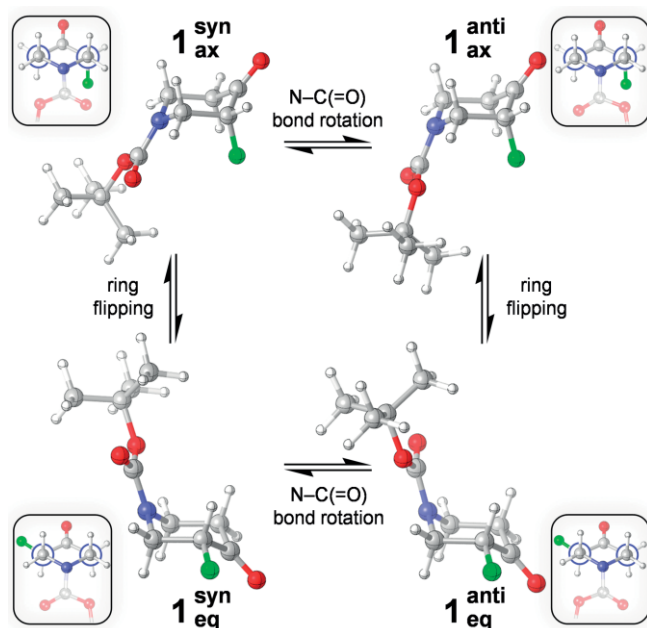


Figure 4. Conformational equilibrium among the four conformers of **1** studied at the B3LYP-D3(BJ)/6-311++G(d,p) level.

Conformational populations according to the Gibbs free energy in the gas phase and in implicit media, using solvents with increasing polarity (namely cyclohexane, chloroform, acetonitrile and DMSO), were calculated to evaluate the influence of the solvent on this conformational equilibrium. The results are shown in the Figure 5. Conformer **1<sub>ax<sup>anti</sup></sub>** is the global energy

minimum (i.e. it has the highest population) in the gas phase, in which the conformational energy increases in the order: **1<sub>ax<sup>anti</sup></sub>** < **1<sub>eq<sup>anti</sup></sub>** < **1<sub>ax<sup>syn</sup></sub>** < **1<sub>eq<sup>syn</sup></sub>**. Thus, there is a preference for the axial fluorine and the orientation **anti** of the Boc group in the gas phase. It is worth mentioning that the energy difference between conformations is small, less than a  $1 \text{ kcal mol}^{-1}$  (the electronic and Gibbs free energies of conformers in all tested media are given in Table S2 of the Supporting Information). The conformational trends change with the inclusion of the solvent. The total axial population (i.e., conformers **1<sub>ax<sup>syn</sup></sub>** and **1<sub>ax<sup>anti</sup></sub>** together) goes from 60 % in the gas phase, 41 % in cyclohexane, 30 % in chloroform to 16 % in acetonitrile and in DMSO. Therefore, when the effect of the solvent is taken into account, the conformational equilibrium gradually shifts towards equatorial conformers. These results can be directly compared to the molecular dipole of the structures ( $\mu = 3.27, 2.63, 3.74$  and  $5.42 \text{ D}$  for the **1<sub>ax<sup>syn</sup></sub>**, **1<sub>ax<sup>anti</sup></sub>**, **1<sub>eq<sup>anti</sup></sub>** and **1<sub>eq<sup>syn</sup></sub>** conformers, respectively), since equatorial conformers have higher molecular dipole moments (therefore, they are more stabilized by polar solvents) than axial conformers.

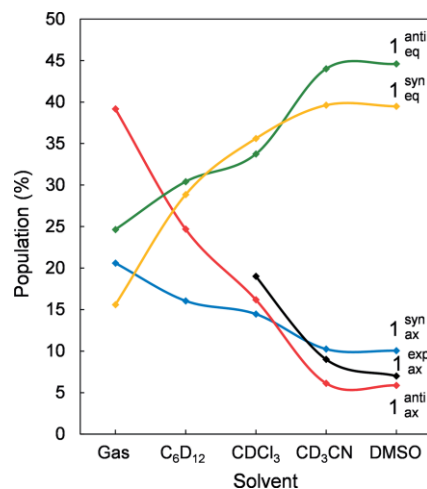


Figure 5. Conformational population according to the Boltzmann distribution of the Gibbs free energies in B3LYP-D3(BJ)/6-311++G(d,p) as a function of the solvent polarity (dipole moment of the solvents increases from the left to the right). Axial population estimated experimentally by NMR (**1<sub>ax<sup>exp</sup></sub>**, black curve) is shown for comparison purposes. (**ax**: axial, **eq**: equatorial, **syn**:  $\varphi_{C-N-C=O} \approx 0^\circ$ , **anti**:  $\varphi_{C-N-C=O} \approx 180^\circ$ ).

To experimentally corroborate these findings, the conformational equilibrium of **1** was evaluated through <sup>1</sup>H NMR studies. The interconversion of one conformation into another usually proceeds quite fast at room temperature, so in the NMR experiments an average signal over all conformers is measured instead of the individual conformers. However, due to the angular dependence of the three-bond hydrogen coupling constant (<sup>3</sup>J<sub>HH</sub>) expressed by the Karplus equation,<sup>[18]</sup> the conformational population of cyclic compounds can be easily estimated by the difference in the <sup>3</sup>J<sub>HH</sub> between axial and equatorial conformers. The <sup>1</sup>H NMR spectra of **1** in the same solvents tested in the theoretical calculations (i.e. cyclohexane, chloroform, acetonitrile and DMSO) are given in the Supporting Information and the spin-spin coupling constants (*J*) are depicted in the Table 1. Because **1** has low solubility in cyclohexane and chloroform, it

was not possible to accurately determine  $J$  in these solvents. Nevertheless, an increase in the  ${}^3J_{\text{HH}}$  can be observed in more polar solvents, which indicates the equatorial preference in solution (because of the greater coupling between axial-axial hydrogens in the equatorial conformer,  $\varphi_{\text{H2-C-C-H3a}} \approx 180^\circ$ , see numbering in the Figure 2), in line with theoretical calculations in implicit solvent.

Table 1. NMR coupling constants ( $J$ , in Hz) obtained experimentally and theoretically for the individual conformers of **1** in implicit solvents at the B3LYP-D3(BJ)/EPR-III level. Estimated axial mole ratios in each media are given in parenthesis.

Conf.	Cyclohexane <sup>[a]</sup>				Chloroform ( $n_{\text{ax}} = 0.20$ )			
	${}^2J_{\text{H2,F}}$	${}^3J_{\text{H2,H3a}}$	${}^3J_{\text{H2,H3e}}$	${}^4J_{\text{H2,H6}}$	${}^2J_{\text{H2,F}}$	${}^3J_{\text{H2,H3a}}$	${}^3J_{\text{H2,H3e}}$	${}^4J_{\text{H2,H6}}$
<b>1<sub>ax</sub><sup>syn</sup></b>	55.8	1.3	3.6	1.1	55.6	1.3	3.6	1.1
<b>1<sub>ax</sub><sup>anti</sup></b>	56.1	1.2	3.6	1.1	55.9	1.2	3.6	1.1
<b>1<sub>eq</sub><sup>anti</sup></b>	53.7	11.2	8.1	1.6	53.7	11.2	8.2	1.7
<b>1<sub>eq</sub><sup>syn</sup></b>	53.3	11.0	8.4	1.6	53.4	11.0	8.5	1.7
<b>Exp.</b>	$\approx 50.0$	n.d. <sup>[a]</sup>	n.d. <sup>[a]</sup>	n.d. <sup>[a]</sup>	48.2	$\approx 9.1$	n.d. <sup>[a]</sup>	n.d. <sup>[a]</sup>

Conf.	Acetonitrile ( $n_{\text{ax}} = 0.10$ )				DMSO ( $n_{\text{ax}} = 0.08$ )			
	${}^2J_{\text{H2,F}}$	${}^3J_{\text{H2,H3a}}$	${}^3J_{\text{H2,H3e}}$	${}^4J_{\text{H2,H6}}$	${}^2J_{\text{H2,F}}$	${}^3J_{\text{H2,H3a}}$	${}^3J_{\text{H2,H3e}}$	${}^4J_{\text{H2,H6}}$
<b>1<sub>ax</sub><sup>syn</sup></b>	55.5	1.3	3.5	1.1	55.5	1.3	3.5	1.1
<b>1<sub>ax</sub><sup>anti</sup></b>	55.7	1.2	3.6	1.2	55.6	1.2	3.6	1.2
<b>1<sub>eq</sub><sup>anti</sup></b>	53.7	11.2	8.3	1.8	53.7	11.2	8.3	1.8
<b>1<sub>eq</sub><sup>syn</sup></b>	53.5	11.0	8.5	1.8	53.5	11.0	8.5	1.8
<b>Exp.</b>	47.5	10.1	6.6	1.1	47.2	10.3	6.7	1.1

[a] Not determined (n.d.) because of the signal broadening attributed to the low solubility in the given media, see  ${}^1\text{H}$  NMR spectra in the Supporting Information.

The  $J$  for the individual conformers (**1<sub>ax</sub><sup>syn</sup>**, **1<sub>ax</sub><sup>anti</sup>**, **1<sub>eq</sub><sup>anti</sup>** and **1<sub>eq</sub><sup>syn</sup>**) was calculated using B3LYP-D3(BJ)/EPR-III (a basis set specifically optimized for coupling constant calculations by DFT<sup>[19]</sup>) and compared with experimental coupling constant ( $J_{\text{obs}}$ ) to estimate the conformational populations using the following Equation (1) and Equation (2):

$$J_{\text{obs}} = n_{\text{ax}}J_{\text{ax}} + n_{\text{eq}}J_{\text{eq}} \quad (1)$$

$$n_{\text{ax}} + n_{\text{eq}} = 1 \quad (2)$$

wherein  $J_{\text{ax}}$  and  $J_{\text{eq}}$  are the individual coupling constants obtained theoretically and  $n_{\text{ax}}$  and  $n_{\text{eq}}$  are the mole ratios of the axial and equatorial conformers, respectively. The results are also shown in the Table 1. The calculated  ${}^2J_{\text{H2F}}$  and  ${}^4J_{\text{H2H6}}$  (see numbering in the Figure 2) agree satisfactorily well with experimental measures ( ${}^2J_{\text{HF}} \approx 50$  Hz and  ${}^4J_{\text{HH}} \approx 1.1$  Hz). The  ${}^3J_{\text{H2H3a}}$  shows the angular dependence in which equatorial and axial conformers have the  ${}^3J_{\text{H2H3a}}$  of ca. 11 Hz and 1 Hz, respectively. The population in each medium was estimated [using Eqs. (1) and (2)] based on an average of the calculated  ${}^3J_{\text{H2H3a}}$  to give the following axial mole ratios (regarding the two axial conformers **1<sub>ax</sub><sup>syn</sup>** and **1<sub>ax</sub><sup>anti</sup>**): 0.20 (chloroform), 0.10 (acetonitrile) and 0.08 (DMSO), black curve in the Figure 5. Therefore, there is a decrease in the axial population on going to more polar media as predicted by the theoretical calculations.

By analyzing the conformational populations of **1**, it seems that the introduction of an endocyclic *N*-Boc group does not significantly change the conformational preferences in the 2-

fluorocyclohexanone backbone. The axial population of **1** in the gas phase is similar to the one reported for the 2-fluorocyclohexanone itself<sup>[1b]</sup> (60 % and 64 %, respectively) and the equatorial conformer is preferred in solution. A similar behavior is observed if the fluorine atom in **1** is replaced by chlorine and bromine (to form **1'** and **1''**, respectively, in Table S3 and Figure S1 of the Supporting Information). These halogens are larger than fluorine and, therefore, conformational changes would be more affected by long-range interactions, if any, in these cases. However, the total axial population of **1'** and **1''** in the gas phase is 88 % and 85 %, respectively, which is quite similar to their 2-halocyclohexanone counterparts (86 % and 92 %, <sup>[1b]</sup> respectively), also highlighting the small effect of the *N*-Boc group on the conformational energies.

Therefore, at a first sight, it was not possible to observe the effect of the orbital interactions expected to be introduced with the *N*-Boc group to further stabilize the axial fluorine conformer. To get more insights on how the *N*-Boc group influences the relative stability of the isolated conformers of **1**, the total electronic energy in the gas phase ( $\Delta E$ ) of each conformer was decomposed within the framework of the Natural Bond Orbital (NBO) analysis<sup>[20]</sup> into three terms: non-Lewis ( $\Delta E_{\text{NL}}$ , which accounts for charge transfer or delocalization energy), Lewis ( $\Delta E_{\text{L}}$ , classical interactions) and dispersion ( $\Delta E_{\text{DISP}}$ , since the electronic energy was calculated using dispersion corrections<sup>[17]</sup>). The NBO results are graphically represented in the Figure 6 (see Table S4 in the Supporting Information for details), where all energy terms are represented relative to the global energy minimum (i.e. conformer **1<sub>ax</sub><sup>anti</sup>**). The  $\Delta E_{\text{DISP}}$  term (yellow curve in Figure 6) has the smallest contribution to the  $\Delta E$  (blue curve) and it is somehow uniform between conformers. The axial conformers (**1<sub>ax</sub><sup>syn</sup>** and **1<sub>ax</sub><sup>anti</sup>**) are in general more stabilized by the  $\Delta E_{\text{L}}$  term (green curve) while equatorial conformers (**1<sub>eq</sub><sup>anti</sup>** and **1<sub>eq</sub><sup>syn</sup>**) are more stabilized by the  $\Delta E_{\text{NL}}$  term (red curve). This trend can be associated with the intramolecular interactions used to explain the conformational energies in 2-fluorocyclohexanone.<sup>[2a,13]</sup> In equatorial conformers, there is a repulsion

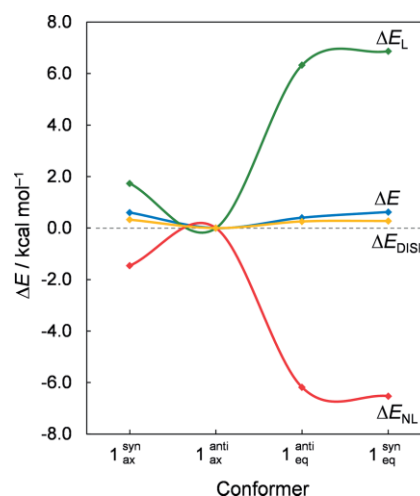


Figure 6. Energy decomposition scheme of the NBO analysis calculated using B3LYP-D3(BJ)/6-311++G(d,p) for the four conformers of **1** (ax: axial, eq: equatorial, **syn**:  $\varphi_{\text{C-N-C=O}} \approx 0^\circ$ , **anti**:  $\varphi_{\text{C-N-C=O}} \approx 180^\circ$ ).

of the fluorine atom with the carbonyl group, as expressed by the less stabilizing  $\Delta E_L$  energy of  $\mathbf{1}_{\text{eq}}^{\text{anti}}$  and  $\mathbf{1}_{\text{eq}}^{\text{syn}}$  (6.33 and 6.87 kcal mol<sup>-1</sup>, respectively), and a greater stabilization from the  $\sigma_{\text{CHax}} \rightarrow \pi^*_{\text{CO}}$  charge transfer, as expressed by the more stabilizing  $\Delta E_{\text{NL}}$  energy (-6.18 and -6.52 kcal mol<sup>-1</sup> for  $\mathbf{1}_{\text{eq}}^{\text{anti}}$  and  $\mathbf{1}_{\text{eq}}^{\text{syn}}$ , respectively).

To estimate the contribution of the hyperconjugative interactions featured in the *gauche* effect to the conformational energies, we looked at the second order perturbation energy [ $E_{i \rightarrow j}^{(2)} = 2F(i,j)^2/(\varepsilon_j - \varepsilon_i)$ ,  $F(i,j)$  is the off-diagonal matrix element,  $\varepsilon_j$  and  $\varepsilon_i$  are the orbital energies<sup>[21]</sup>] in the NBO analysis that estimates delocalization energies from orbital interactions (Table S5 of the Supporting Information). The  $\sigma_{\text{CH}} \rightarrow \sigma^*_{\text{CF}}$  and  $\sigma_{\text{CH}} \rightarrow \sigma^*_{\text{CN}}$  antiperiplanar interactions (4.6 and 2.9 kcal mol<sup>-1</sup>, respectively) in the *gauche* orientation (i.e. in the axial conformers) are indeed more stabilizing than the corresponding  $\sigma_{\text{CH}} \rightarrow \sigma^*_{\text{CH}}$  and  $\sigma_{\text{CF/CN}} \rightarrow \sigma^*_{\text{CN/CF}}$  interactions (2.3, 1.1 and 1.8 kcal mol<sup>-1</sup>, respectively) in the *anti*-orientation (i.e. in the equatorial conformers). However, equatorial conformers are still more stabilized by the  $\Delta E_{\text{NL}}$  term, so it seems that these orbital interactions are not stabilizing enough to change the equilibria towards axial conformers as first expected. The  $\sigma_{\text{CHax}} \rightarrow \pi^*_{\text{CO}}$  charge transfer in equatorial conformers, on the other hand, accounts for 6.7 kcal mol<sup>-1</sup> (Table S5), which is more stabilizing than the abovementioned interactions in the axial conformers and explains the trends in  $\Delta E_{\text{NL}}$ . The main orbital interactions are schematically represented in the Figure S2 of the Supporting Information.

The *N*-Boc is a bulky group though, so it might introduce factors other than the *gauche* effect that influence the fluorine axial–equatorial preference. Thus, to simplify the system and get more insight on the role of specific structural parts, the relative energies of  $\mathbf{1}$  were also compared with other 2-fluorocyclohexanone analogs (Figure 7).  $\mathbf{2}$  and  $\mathbf{3}$  were chosen as to gradually reduce the *N*-Boc group and to evaluate the role of specific structural parts on the conformational energies. The

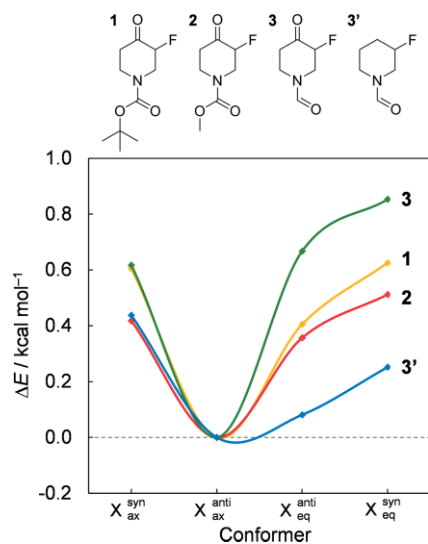


Figure 7. Relative conformational energies for the 2-fluorocyclohexanone analogs, where  $\mathbf{X} = \mathbf{1}$ – $\mathbf{3}$ . (**ax**: axial, **eq**: equatorial, **syn**:  $\varphi_{\text{C-N-C=O}} \approx 0^\circ$ , **anti**:  $\varphi_{\text{C-N-C=O}} \approx 180^\circ$ ), computed at the B3LYP-D3(BJ)/6-311++G(d,p) level.

conformers of all analogs were named in the same manner as for  $\mathbf{1}$ , to distinguish the two orientations of the N–C=O group (**syn** and **anti**,  $\varphi_{\text{C-N-C=O}} \approx 0^\circ$  and  $180^\circ$ , respectively) and axial or equatorial fluorine (**ax** and **eq**, respectively). Schematic representation of the conformers of analogs  $\mathbf{2}$  and  $\mathbf{3}$  is given in Figure S1 of the Supporting Information.

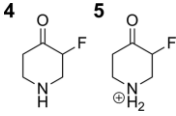
According to Figure 7, the energy trends of analogs  $\mathbf{2}$  and  $\mathbf{3}$  are quite similar to  $\mathbf{1}$  (also regarding the energy trends in the NBO analysis, Table S3 in the Supporting Information). The  $\mathbf{X}_{\text{ax}}^{\text{anti}}$  is the global energy minimum and the conformational energy increases in the order:  $\mathbf{X}_{\text{ax}}^{\text{anti}} < \mathbf{X}_{\text{eq}}^{\text{anti}} \approx \mathbf{X}_{\text{ax}}^{\text{syn}} < \mathbf{X}_{\text{eq}}^{\text{syn}}$ . Due to the overall similarity in the energy trends on going from  $\mathbf{1}$  to  $\mathbf{3}$ , i.e. on removing the *t*Bu group and the oxygen atom linked to it from the Boc group (Figure 7), it was possible to reduce the influence of the *N*-Boc group on the conformational stability of  $\mathbf{1}$  to the amide group of analog  $\mathbf{3}$ . Therefore, to specifically search for the *gauche* effect, the interaction between this amide group with the fluorine atom, without the influence of the ketone group (compound  $\mathbf{3}'$  in Figure 7), was then evaluated. The removal of the carbonyl group to form  $\mathbf{3}'$  leads to a decrease in the relative energies among conformers (Figure 7). In this case, the orientation of the amide group is more relevant for the conformational energies than the orientation of the fluorine atom. Conformers  $\mathbf{3}'_{\text{ax}}^{\text{anti}}$  and  $\mathbf{3}'_{\text{eq}}^{\text{anti}}$  have nearly the same total energy, and the energy difference between  $\mathbf{3}'_{\text{ax}}^{\text{syn}}-\mathbf{3}'_{\text{ax}}^{\text{anti}}$  and  $\mathbf{3}'_{\text{eq}}^{\text{syn}}-\mathbf{3}'_{\text{eq}}^{\text{anti}}$  is 0.44 and 0.17 kcal mol<sup>-1</sup>, respectively. The energy difference is more significant for the axial fluorine probably due to the closer proximity with the amide carbonyl oxygen in  $\mathbf{3}'_{\text{ax}}^{\text{syn}}$  (see Figure S1). Additionally, the  $\Delta E_{\text{NL}}$  and  $\Delta E_L$  terms from the NBO analysis have opposite trends compared to  $\mathbf{1}$ – $\mathbf{3}$  (Table S3). With the removal of the carbonyl group, the  $\sigma_{\text{CH}} \rightarrow \pi^*_{\text{CO}}$  charge transfer and  $F_{\text{eq}}/\text{C=O}$  repulsion used to explain the conformational stability of the 2-fluorocyclohexanone are cancelled out. Now axial conformers are more favored by the  $\Delta E_{\text{NL}}$  term, which can be related to the orbital interactions featured in the *gauche* effect, and less favored by the  $\Delta E_L$  term relative to equatorial conformers, due to the removal of the  $F_{\text{eq}}/\text{C=O}$  repulsion and also to a possible incremental repulsion of the axial fluorine with the amide group.

Differently from other structures containing the fluoroethylamide fragment,<sup>[7]</sup> a stereoelectronic stabilization in the *gauche* arrangement is not the determining factor in the conformational behavior of the 2-fluorocyclohexanone analogs analyzed herein. Even without the influence of the ketone group in  $\mathbf{3}'$ , the energy difference between axial and equatorial conformers (*gauche* and *anti*, respectively) is too small to observe any substantial stabilization due to the *gauche* effect. Earlier reports in the literature<sup>[13,22]</sup> have evaluated other endocyclic groups at the same position of the 2-fluorocyclohexanone backbone known to induce the *gauche* effect in acyclic compounds (e.g.  $\text{X} = \text{O}^{[13]}$  and  $\text{S}^{[22]}$ ). However, in all cases the conformational trends could not be attributed to hyperconjugation. It seems that the orbital interactions used to explain the preferred *gauche* orientation in acyclic compounds are, surprisingly, not strong enough to dictate the conformational preferences in heterocycles. Instead, conformational preferences of the 2-fluoro-

cyclohexanone analogs are primarily affected by a short-range interaction with the ketone group.

To counterbalance the effect of the carbonyl group on the axial–equatorial equilibrium it is necessary to add an endocyclic group which can induce a stronger intramolecular interaction, probably electrostatic in nature. Thus, if the *N*-Boc group is continuously reduced to form analog **4** (which possesses only a hydrogen attached to the nitrogen atom, resembling part of the active nucleus of a 4-quinolone), then one can see a totally different trend (Table 2, see Table S3 in the Supporting Information for details). The conformational analysis of **4** has already been reported in the literature,<sup>[22]</sup> where the stability of the global energy minimum (which have both fluorine and *N*-hydrogen atoms in the axial, **4<sub>F-ax</sub><sup>H-ax</sup>** in Figure S1) is attributed to an N–H<sup>δ+</sup>...<sup>δ-</sup>F electrostatic interaction (in line with our NBO results in Table S3). This effect becomes stronger by protonating the amine group (to form analog **5**, the 3-fluoro-4-oxopiperidin-1-ium cation, in Table 2; schematic representation in Figure S1). In this case, the axial fluorine persists even in highly polar solvents, such as DMSO (Table 2), similar to the results reported for the 3-fluoropiperidinium cation that have been attributed to the so-called electrostatic *gauche* effect.<sup>[14d,23]</sup>

Table 2. Relative conformational energies (in kcal mol<sup>-1</sup>) for the 2-fluorocyclohexanone analogs **4** and **5**, in gas phase and DMSO, computed at the B3LYP–D3(BJ)/6-311++G(d,p) level.



<b>4</b>			<b>5</b>		
Conf.	gas	DMSO	Conf.	gas	DMSO
<b>4<sub>F-ax</sub><sup>H-ax</sup></b>	0.0	1.1	<b>5<sub>F-ax</sub></b>	0.0	0.0
<b>4<sub>F-ax</sub><sup>H-eq</sup></b>	2.4	2.8			
<b>4<sub>F-eq</sub><sup>H-ax</sup></b>	1.6	0.0			
<b>4<sub>F-eq</sub><sup>H-eq</sup></b>	1.4	0.8	<b>5<sub>F-eq</sub></b>	5.4	0.3

## Conclusion

The conformational preferences of **1** predicted by DFT calculations nicely reproduce the trends in the NMR experiments. There is an increase in the population of equatorial conformers on going from nonpolar to increasingly more polar solvents, as evidenced by the analysis of the <sup>3</sup>J<sub>HH</sub> coupling constant. The conformational trends of **1** are quite similar to that of 2-fluorocyclohexanone itself (the same is observed for other 2-halocyclohexanones). The introduction of the endocyclic *N*-Boc group does not result in a significant stabilization of the axial fluorine due to interactions responsible for the *gauche* effect; the stabilization from hyperconjugative interactions featured in the *gauche* effect is overcome by the charge transfer from the σ<sub>CHax</sub> occupied orbital to the π\*<sub>CO</sub> empty orbital in the equatorial conformers. Through comparison with analogs **2–5**, it is possible to assess the influence of specific structural parts to the relative energies. The axial–equatorial equilibrium of the heterocycles analyzed herein is primarily dictated by the ketone group

of the 2-fluorocyclohexanone backbone; however, an endocyclic group inducing strong electrostatic interactions shifts the conformational preferences. Given the widely applicability of organofluorine compounds, understanding the factors ruling their molecular structure can assist the design of novel compounds with improved molecular properties.

## Experimental Section

Commercial samples of 1-Boc-3-fluoro-4-oxopiperidine (**1**) were purchased and used without further purification. The <sup>1</sup>H NMR spectra were acquired at 499.99 MHz from 2.0 mg mL<sup>-1</sup> solution of **1** in the appropriate solvents (i.e. C<sub>6</sub>D<sub>12</sub>, CDCl<sub>3</sub>, CD<sub>3</sub>CN and [D<sub>6</sub>]DMSO) in standard 5 mm glass tubes. A direct observation probe was employed, and the probe temperature was set to 298.1 K. The 90° observation pulses were previously calibrated and had typical durations of 11.75 μs.

**Computational Details:** The energy profile of rotation around the φ<sub>C–N–C=O</sub> dihedral angle for axial and equatorial conformers of **1** was obtained with a step size of 30° at the MP2/6-311++G(d,p) level. The geometries of the located energy minima of **1** were then optimized using density functional methods, namely the ωB97X–D, B3LYP and M062X hybrid functionals and the B97–D and BLYP functionals with the 6-311++G(d,p) basis set,<sup>[15b]</sup> in order to determine the appropriate level of theory for the system in study. Dispersion effects were considered by the dispersion corrections proposed by Grimme et al. with the BJ damping function<sup>[17]</sup> and MP2 was used as the reference method. B3LYP–D3(BJ) was selected because, among the density functionals with the smallest MAE value, it better reproduces the trends in the conformational population compared to MP2 (see Table S1). Frequency calculations were performed to obtain thermodynamic energies and to ensure that structures converged to true energy minima. The role of solvent effects on this conformational equilibrium was assessed by geometry optimization and frequency calculations in implicit solvents (cyclohexane, chloroform, acetonitrile and DMSO) according to the integral equation formalism variant of the Polarizable Continuum Model (IEFPCM).<sup>[24]</sup> The NBO analysis<sup>[20]</sup> was used to search for prospective intramolecular interactions influencing conformational energies. All calculations were performed using the previously selected level of theory. Additionally, calculations of the spin–spin coupling constants (also in cyclohexane, chloroform, acetonitrile and DMSO) using the *gauge including atomic orbital* (GIAO) method<sup>[25]</sup> with the EPR–III basis set<sup>[19]</sup> were performed and compared with experimental NMR spectra in order to estimate the relative conformer population in each media. All abovementioned calculations were carried out using the Gaussian 09 rev. D01 program<sup>[26]</sup> and molecular structures were illustrated using CYLview.<sup>[27]</sup>

## Acknowledgments

The authors acknowledge the Conselho Nacional de Desenvolvimento Científico e Tecnológico (CNPq) for the scholarships to D.R. S. and L.A. Z. (grant numbers 140955/2017-8 and 142476/2018-8, respectively) and the fellowship to M.P. F. (grant number 301371/2017-2), the Coordenação de Aperfeiçoamento de Pessoal de Nível Superior (CAPES) for the visiting student scholarship to D.R. S. (grant number 88881.190436/2018-01), the Fundação de Amparo à Pesquisa do Estado de Minas Gerais (FAPEMIG, grant numbers CEX–APQ–00383/15 and CEX–APQ–

00344/17), as well as the Netherlands Organization for Scientific Research (NWO) for the financial support.

**Keywords:** Axial–equatorial equilibrium · Conformation analysis · Fluorine gauche effect · Heterocycles · Stereoelectronic effects

- [1] a) N. L. Allinger, H. M. Blatter, *J. Org. Chem.* **1962**, *27*, 1523; b) F. Yoshinaga, C. F. Tormena, M. P. Freitas, R. Rittner, R. J. Abraham, *J. Chem. Soc., Perkin Trans. 2* **2002**, *0*, 1494.
- [2] a) J. V. Coelho, M. P. Freitas, *THEOCHEM* **2010**, *941*, 53; b) C. F. Tormena, *Prog. Nucl. Magn. Reson. Spectrosc.* **2016**, *96*, 73.
- [3] a) L. Hunter, *Beilstein J. Org. Chem.* **2010**, *6*, 1; b) D. O'Hagan, *J. Org. Chem.* **2012**, *77*, 3689.
- [4] L. Goodman, H. Gu, V. Pophristic, *J. Phys. Chem. A* **2005**, *109*, 1223.
- [5] a) I. V. Alabugin, K. M. Gilmore, P. W. Peterson, *Wiley Interdiscip. Rev.: Comput. Mol. Sci.* **2011**, *1*, 109; b) C. Thiehoff, Y. P. Rey, R. Gilmour, *Isr. J. Chem.* **2017**, *57*, 92.
- [6] D. Y. Buissonneaud, T. Van Mourik, D. O'Hagan, *Tetrahedron* **2010**, *66*, 2196.
- [7] a) D. O'Hagan, C. Bilton, J. A. K. Howard, L. Knight, D. J. Tozer, *J. Chem. Soc., Perkin Trans. 2* **2000**, *0*, 605; b) C. R. S. Briggs, D. O'Hagan, J. A. K. Howard, D. S. Yufit, *J. Fluorine Chem.* **2003**, *119*, 9.
- [8] a) Y. P. Rey, L. E. Zimmer, C. Sparr, E. M. Tanzer, W. B. Schweizer, H. M. Senn, S. Lakhdar, R. Gilmour, *Eur. J. Org. Chem.* **2014**, *2014*, 1202; b) M. Aufiero, R. Gilmour, *Acc. Chem. Res.* **2018**, *51*, 1701.
- [9] C. S. Teschers, C. G. Daniliuc, G. Kehr, R. Gilmour, *J. Fluorine Chem.* **2018**, *210*, 1.
- [10] S. Paul, W. B. Schweizer, G. Rugg, H. M. Senn, R. Gilmour, *Tetrahedron* **2013**, *69*, 5647.
- [11] G. Pattison, *Beilstein J. Org. Chem.* **2017**, *13*, 2915.
- [12] J. I. Seeman, *Chem. Rev.* **1983**, *83*, 83.
- [13] T. F. B. Silva, L. A. F. Andrade, J. M. Silla, C. J. Duarte, R. Rittner, M. P. Freitas, *J. Phys. Chem. A* **2014**, *118*, 6266.
- [14] a) R. Koudih, G. Gilbert, M. Dhilly, A. Abbas, L. Barré, D. Debruyne, F. Sobrio, *Eur. J. Med. Chem.* **2012**, *53*, 408; b) Y. Nakajima, T. Inoue, K. Nakai, K. Mukoyoshi, H. Hamaguchi, K. Hatanaka, H. Sasaki, A. Tanaka, F. Takahashi, S. Kunikawa, H. Usuda, A. Moritomo, Y. Higashi, M. Inami, S. Shirakami, *Bioorg. Med. Chem.* **2015**, *23*, 4871; c) B. Planty, C. Pujol, M. Lamothe, C. Maraval, C. Horn, B. Le Grand, M. Perez, *Bioorg. Med. Chem. Lett.* **2010**, *20*, 1735; d) A. Sun, D. C. Lankin, K. Hardcastle, J. P. Snyder, *Chem. Eur. J.* **2005**, *11*, 1579.
- [15] a) M. Head-Gordon, J. A. Pople, M. Frisch, *Chem. Phys. Lett.* **1988**, *153*, 503; b) R. Krishnan, J. S. Binkley, R. Seeger, J. A. Pople, *J. Chem. Phys.* **1980**, *72*, 650.
- [16] a) A. D. Becke, *Phys. Rev. A* **1988**, *38*, 3098; b) C. Lee, W. Yang, R. G. Parr, *Phys. Rev. B* **1988**, *37*, 785.
- [17] S. Grimme, S. Ehrlich, L. Goerigk, *J. Comput. Chem.* **2011**, *32*, 1456.
- [18] a) M. Karplus, *J. Chem. Phys.* **1959**, *30*, 11; b) M. Karplus, *J. Phys. Chem.* **1960**, *64*, 1793; c) M. Karplus, *J. Am. Chem. Soc.* **1963**, *85*, 2870.
- [19] V. Barone, in *Recent Adv. Density Funct. Methods*, Part I (Ed.: D. P. Chong), World Scientific Publ. Co., Singapore, **1996**.
- [20] a) E. D. Glendening, J. K. Badenhop, A. E. Reed, J. E. Carpenter, J. A. Bohmann, C. M. Morales, C. R. Landis, F. Weinhold, *NBO 6.0*. Theoretical Chemistry Institute, University of Wisconsin, Madison, **2013**; b) E. D. Glendening, C. R. Landis, F. Weinhold, *J. Comput. Chem.* **2013**, *34*, 1429.
- [21] F. Weinhold, C. R. Landis, E. D. Glendening, *Int. Rev. Phys. Chem.* **2016**, *35*, 399.
- [22] F. A. Martins, J. M. Silla, M. P. Freitas, *Beilstein J. Org. Chem.* **2017**, *13*, 1781.
- [23] J. M. Silla, W. G. D. P. Silva, R. A. Cormanic, R. Rittner, C. F. Tormena, M. P. Freitas, *J. Phys. Chem. A* **2014**, *118*, 503.
- [24] J. Tomasi, B. Mennucci, R. Cammi, *Chem. Rev.* **2005**, *105*, 2999.
- [25] a) K. Wolinski, J. F. Hinton, P. Pulay, *J. Am. Chem. Soc.* **1990**, *112*, 8251; b) R. Ditchfield, *J. Chem. Phys.* **1972**, *56*, 5688.
- [26] M. J. Frisch, G. W. Trucks, H. B. Schlegel, G. E. Scuseria, M. A. Robb, J. R. Cheeseman, G. Scalmani, V. Barone, B. Mennucci, G. A. Petersson, H. Nakatsuji, M. Caricato, X. Li, H. P. Hratchian, A. F. Izmaylov, J. Bloino, G. Zheng, J. L. Sonnenberg, M. Hada, M. Ehara, K. Toyota, R. Fukuda, J. Hasegawa, M. Ishida, T. Nakajima, Y. Honda, O. Kitao, H. Nakai, T. Vreven, J. A. Montgomery Jr., J. E. Peralta, F. Ogliaro, M. Bearpark, J. J. Heyd, E. Brothers, K. N. Kudin, V. N. Staroverov, R. Kobayashi, J. Normand, K. Raghavachari, A. Rendell, J. C. Burant, S. S. Iyengar, J. Tomasi, M. Cossi, N. Rega, J. M. Millam, M. Klene, J. E. Knox, J. B. Cross, V. Bakken, C. Adamo, J. Jaramillo, R. Gomperts, R. E. Stratmann, O. Yazyev, A. J. Austin, R. Cammi, C. Pomelli, J. W. Ochterski, R. L. Martin, K. Morokuma, V. G. Zakrzewski, G. A. Voth, P. Salvador, J. J. Dannenberg, S. Dapprich, A. D. Daniels, Ö. Farkas, J. B. Foresman, J. V. Ortiz, J. Cioslowski, D. J. Fox, *Gaussian 09*, Revision D.01; Gaussian, Inc., Wallingford CT, **2013**.
- [27] C. Y. Legault, *CYLVIEW 1.0b*. University of Sherbrooke, Sherbrooke, **2009**.

Received: December 10, 2019